ORIGINAL ARTICLE

On-the-fly laser processing method with high efficiency for continuous large-scale trajectories

Tieshuang Zhu[1,2] · **Shuai Ji**[1,2] · **Chengrui Zhang**[1,2] · **Yisheng Yin**[1,2]

Abstract

Laser processing with galvanometric scanners and servo platforms has been prosperous in the industry recently, and researches in this field have been evolved from step-and-scan methods to on-the-fly methods. However, the major on-the-fly methods only consider the high dynamic performance of the scanner and waste the characteristic of the scanner working area. This study proposes a new method that utilizes both above to improve efficiency conspicuously without loss of accuracy, aiming at continuous large-scale trajectories. In this method, the decomposed trajectories for the platform are derived from the target trajectories geometrically, and interpolation for the scanner trajectories is implemented through vector subtraction of positions. The experimental results with the given patterns indicate that the total processing time of the proposed method is shortened by 67.3% compared with the traditional step-and-scan method and 51.4% compared with the major on-the-fly method. Meanwhile, motion performance is better, fewer defects appear, and all detected errors satisfy the requirement. In conclusion, the proposed on-the-fly method combines efficiency and quality, thus perfectly suiting industrial laser processing applications.

Keywords On-the-fly laser processing · Galvanometric scanner · Continuous large-scale trajectory · Trajectory decomposition · Optimal time

1 Introduction

The on-the-fly laser processing system, typically consisting of a laser generator and a multi-axis mechanism with a two/three-axis galvanometric scanner as its end-effector, has a tremendous tendency towards utilization in wide-spread industries, especially in high-end manufacturing. During processing, the scanner is guided by the drive mechanism and moves at a focal distance perpendicular to the processing surface, which exactly looks like it is flying along the tool path. On-the-fly laser processing takes advantages of both laser galvanometer scanning and servo platform motion, such as high efficiency and accuracy, no contact stress and small heat-affected zone in processing, various material compatibility, and flexibility of automation. In some researches, on-the-fly laser processing systems have been alternatively identified as macro-and-micro manipulators or kinematically redundant mechanisms [1]. Applications of on-the-fly laser processing are prosperous in practical aspects due to its high performance and product quality [2–6], e.g., polishing, ablation, welding, marking/engraving, hole drilling, cutting, surface texturing, and additive manufacturing.

Generally, the recent researches of laser processing with galvanometric scanners can be divided into two categories—fragmented/small areas [7, 8] and continuous/large areas [9, 10], based on the processed patterns. As for fragmented/small areas, the servo-driven platform functions as a coarse locator initially and the galvanometric scanner functions as a fine locator subsequently, which means no coordination or synchronization between the platform and the scanner is needed. However, as for continuous/large areas, the platform and the scanner must cooperate and function simultaneously in order to achieve the specific patterns, which requires

✉ Shuai Ji
  jishuai@sdu.edu.cn

✉ Chengrui Zhang
  sduzcr@126.com

1 School of Mechanical Engineering, Shandong University, Jinan 250061, China

2 Key Laboratory of High Efficiency and Clean Mechanical Manufacture, School of Mechanical Engineering, Shandong University, Jinan 250061, China

higher level of accuracy in both positioning and synchronizing. Sincerely, the research on trajectory generation and time optimization of continuous/large areas is the focus in this study, which has become highlights and hotspots in laser processing recently.

Dividing a large area into small regions and scanning these regions sequentially, namely, a step-and-scan method [9–11], was a feasible strategy in earlier studies to achieve entire processing trajectories much larger than the working area of the galvanometric scanner. However, this strategy leads to low productivity and discontinuity defects such as stitching error [11] and overburn. An on-the-fly processing method in which galvanometers with fast dynamic response and a servo platform with a large range of motion can move and process the trajectories simultaneously is another novel strategy to solve the above problems. The key point of the on-the-fly method is decomposition of the target trajectory, which generates trajectories of the platform and the galvanometric scanner respectively, under the constrains of platform acceleration and scanner working area. The purpose of this method is basically to smooth out the motion of the servo platform, allowing the scanner accomplish high-frequency aspects of motion, such as sharp corners. Numerous researchers have done work about this. Kim et al. [9] used a parabolic shape to minimize platform acceleration/deceleration when processing corner lines. Erkorkmaz et al. [12] applied an acceleration-continuous cubic spline in on-the-fly drilling to improve motion smoothness and productivity. Yoon et al. [13] proposed a GCD (grid cell decomposition) algorithm in on-the-fly marking, in which an entire area was divided into functional grids and then processing paths were calculated. Alzaydi [14, 15] illustrated parameterized-spline toolpath planning and trapezoidal interpolation in on-the-fly drilling and optimized them for each machine axis by

minimal values of integral square of jerk. Cui et al. [11] developed a synchronized control system with a motion decomposition module using a moving average low-pass filter, while Uzunoglu et al. [1] also utilized a filtering function to derive platform's motion. In summary, those methods concentrate merely on smoothening trajectories, but the discrepancy between the target motion and the decomposed platform motion is unnoticeable and much smaller than the working area of the scanner. In other words, regarding laser galvanometric scanners, the advantages of high dynamic performance are fully highlighted, but the potential advantages of working area scale are completely ignored.

This study proposes a new motion decomposition method for on-the-fly laser processing, aiming to achieve continuous large-scale trajectories. Preliminary trajectories are obtained by specified geometric criteria associated with the working area scale of the galvanometric scanner, and secondary trajectories performed by the servo platform are generated by replacing corners with transitional arcs associated with the maximal acceleration of the servo platform. After interpolation, scanner positions are calculated in real-time context by making vector subtraction of the platform positions from the target positions. The proposed method is experimentally compared with the step-and-scan method in terms of efficiency and accuracy.

2 Methods

An on-the-fly laser processing system is generally composed of a servo-driven platform, a galvanometric scanner, a laser generator, and other auxiliary modules. Figure 1 shows a typical structure of a planar on-the-fly laser processing

Fig. 1 A schema of a planar on-the-fly laser processing system
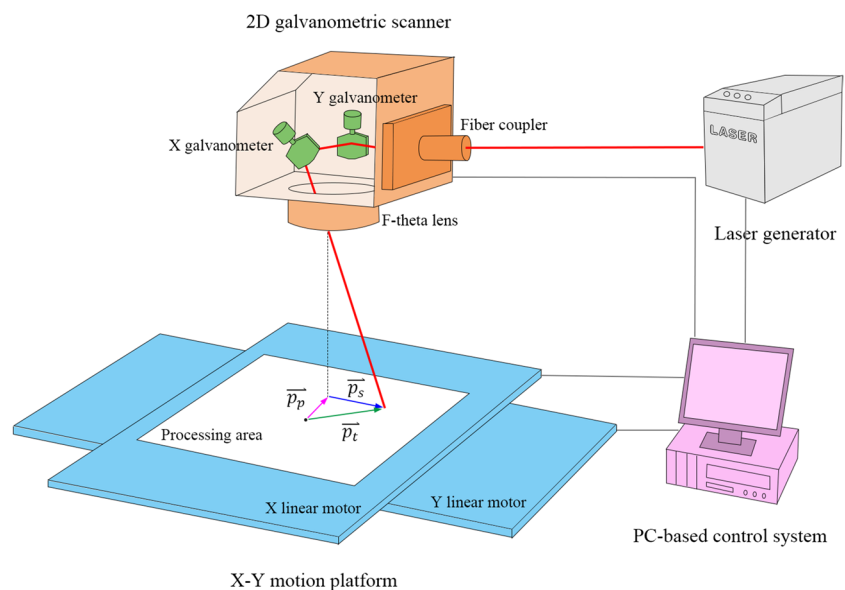
machine, where the target position $\vec{p_t}$ is a vector addition of the platform position $\vec{p_p}$ and the scanner position $\vec{p_s}$:

$$\vec{p_t} = \vec{p_p} + \vec{p_s} \tag{1}$$

Most on-the-fly laser processing systems have redundancy in DOF (degree of freedom) which can cause issues with inverse kinematics and optimization. It is important to bear in mind certain conditions when dealing with the unavoidable decomposition of target trajectories:

- The dynamic performance (i.e., maximal velocity and maximal acceleration) of the galvanometric scanner is much greater than that of the servo platform.
- The motion range (in both X and Y) of the galvanometric scanner is smaller than that of the servo platform.
- The generated trajectories for the motion of the servo platform should be as short as possible in length and as smooth as possible to optimize the processing time.

The preliminary trajectories are extracted from the original target trajectories to reduce the overall length by sufficiently utilizing the scanner working area, as shown in Fig. 2. The radius of the scanner's recommended working area is regarded as R_0, some detailed steps are demonstrated as follows:

1) Make an interior angular bisector at the intersection P of the two segments (consider the tangent if there is a curve, Fig. 2b).

2) Take a characteristic point T on the angular bisector so that the length of PT equals R_0 (Fig. 2a, b).
3) Connect all the characteristic points $T_1, T_2, \ldots, T_n$ of the intersections $P_1, P_2, \ldots, P_n$ in sequence (Fig. 2c) to get the preliminary trajectories.

To concisely prove that the preliminary trajectories have the shortest length under the working area constraints of the scanner, a localized corner (Fig. 3a) is selected from the continuous large-scale trajectories (Fig. 3b). The characteristic point T is on the circle with P as the center and R_0 as the radius. A and C are the intersections of the original corner and the circle, B and D are the intersections of the preliminary corner and the tangents of arc AC, and E is the self-intersection of the tangents. Assuming that the distance between adjacent corners is as far as possible to simplify the proof, the segment between points A of two adjacent corners is almost parallel and equivalent to the segment between points B of two adjacent corners, as the same situation as points C and D. That is, in the case of Fig. 3, AA_1 is almost parallel and equivalent to BB_1, and CC_2 is almost parallel and equivalent to DD_2. Therefore, only the patterns in the quadrilateral $PAEC$ need to be concerned.

Symbols are interpreted as follows:

- γ is the interior angle of the corner, $\gamma \in [0, \pi]$.
- θ is the variable angle between PA and PT, $\theta \in [0, \gamma]$.
- a is the perpendicular distance from point T to line AE.
- b is the perpendicular distance from point T to line CE.

Fig. 2 Preliminary trajectory generation in **a, b** corner view and **c** full view. Black marks the original target trajectories, red marks the preliminary trajectories, and blue marks the working area of the scanner
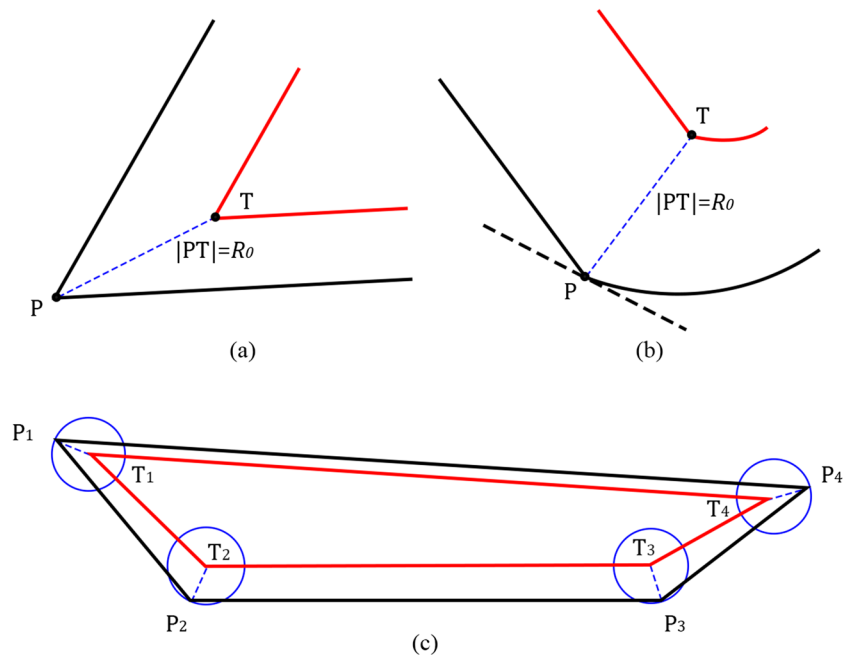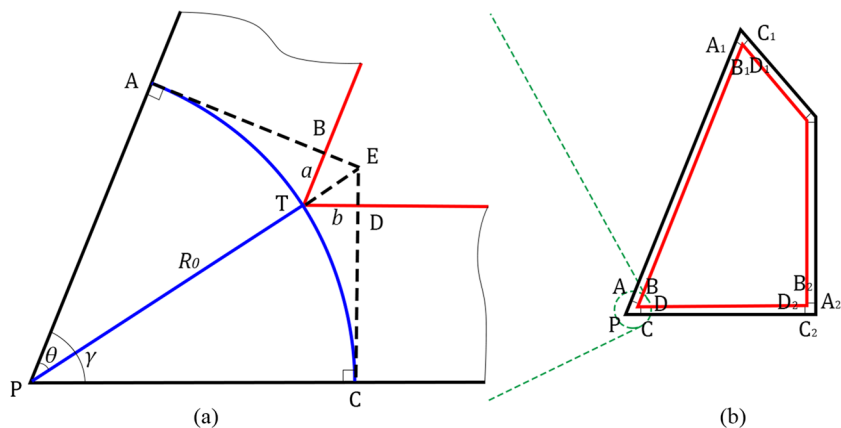
(a)   (b)

To get the optimal position of T, the extremum of function $f(\theta) = a + b$ needs to be determined. In geometry, a and b are calculated respectively as follows:

$$a = \cos\theta\left(\frac{R_0}{\cos\theta} - R_0\right) = R_0(1 - \cos\theta) \tag{2}$$

$$b = \cos(\gamma - \theta)\left[\frac{R_0}{\cos(\gamma - \theta)} - R_0\right] = R_0[1 - \cos(\gamma - \theta)] \tag{3}$$

Thus,

$$f(\theta) = a + b = 2R_0 - R_0[\cos\theta + \cos(\gamma - \theta)] \tag{4}$$

$$f'(\theta) = R_0[\sin\theta - \sin(\gamma - \theta)] \tag{5}$$

It can be seen that $f(\theta)$ reaches the extremum value (local minimum) when $\theta = \gamma/2$, i.e., T is on the interior angular bisector of the corner.

Based on the preliminary trajectories, the corners (C_0 continuity, C_1 discontinuity) are replaced with transitional arcs (C_0 continuity, C_1 continuity) in order to smoothen the trajectories and decrease the acceleration/deceleration time of the platform motion, which leads to secondary (final) trajectories, as shown in Fig. 4. Considering the centripetal acceleration should not exceed the maximal acceleration of the platform, the radius of transitional arc, r_0 is determined as follows:

Fig. 4 Secondary trajectories in **a** full view and **b** corner view after the process of Fig. 2c. **c** A schema of interpolation. Black marks the target trajectories, red marks the platform trajectories, and blue marks the vectors of scanner position

(a)

(b)   (c)
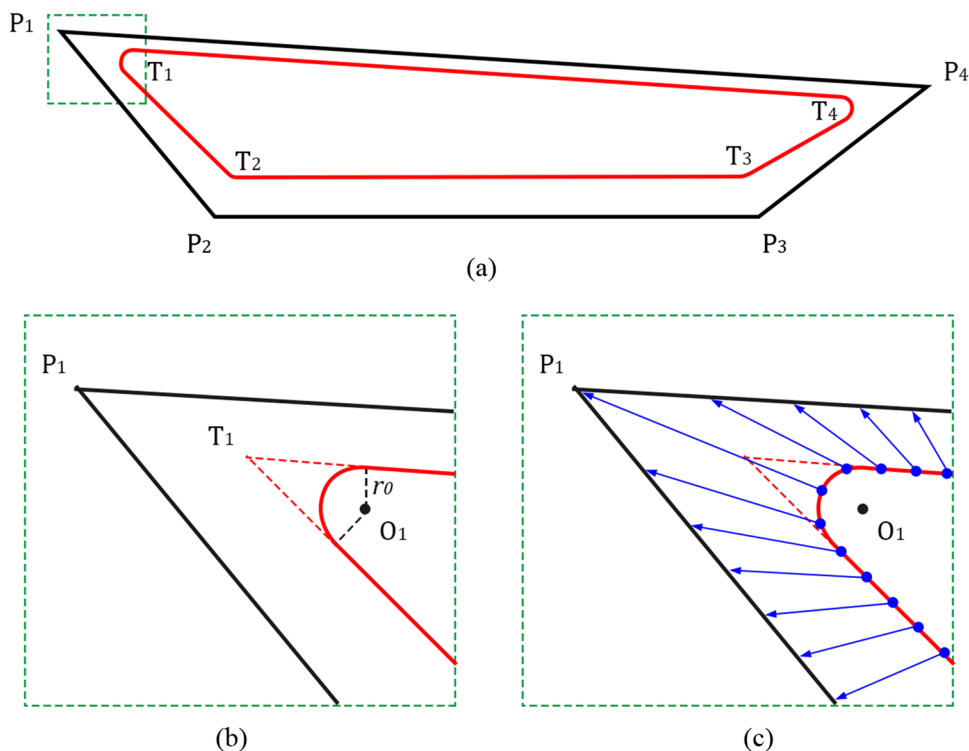
$$r_0 = \frac{v_p^2}{a_{\max}} \qquad (6)$$

where v_p is the working velocity and $a_{\max}$ is the maximal acceleration/deceleration of the servo platform.

In practice, the platform moves along the secondary trajectories at the velocity of v_p and the scanner compensates the residual displacement (Fig. 4c) according to Eq. 1 to complete the entire laser processing. The proposed method has several advantages. A geometric solution instead of a numerical or iterative one relieves the calculative burden of the control system, especially in a real-time context. Moreover, as for the platform, the overall length of the motion is smaller and less deceleration occurs during processing, which saves plenty of time.

3 Experimental results and discussion

An experimental setup for on-the-fly laser processing is shown in Fig. 5a. In experiments, a pulsed fiber laser generator with a central wavelength of 1064 nm was utilized as a processing tool to mark the designed patterns on black photographic papers. The laser generator applies 100 ns pulse width with frequency set to 50 kHz and has a maximal power output of 20 W with instability of 3%. The quality of output laser beam (M^2) is 1.4. In addition, a three-axis servo platform was implemented, where X/Y axes are driven by linear motors with working area capability of 300×300 mm², and Z axis is driven by a servo motor and a ball screw to adjust defocus distance. The positioning accuracy of the linear platform is measured to be 60 μm. The Z axis remains fixed when processing some planar workpieces remarkably. Furthermore, a 2D galvanometric scanner played a key role in the on-the-fly laser processing experiments. It has a maximum working area of 90×90 mm², and its f-theta lens has a focal length of 210 mm. The maximal scanning velocity of the scanner is 3 m/s. After experiments, the processed samples were observed and measured using the VMA Video Measuring Machine from TZTEK, as shown in Fig. 5b.

On-the-fly laser experiments were carried out to analyze the efficiency, accuracy, and processing quality of the proposed method in comparison to the step-and-scan method and the major on-the-fly method. A pattern combining a star and a circle (Fig. 6a) was designed as the target trajectories to validate the above performance. The size of the pattern was 180×180 mm². R_0 was set to 45 mm. According to Eq. 6, r_0 was calculated as 4 mm, since v_p was 100 mm/s and $a_{\max}$ was 2500 mm/s².

Three experimental groups were categorized by three processing methods: the step-and-scan method, the on-the-fly method using arc transition only, and the on-the-fly method using both geometric shrinkage and arc transition. In this study, the on-the-fly method only using arc transition represents the major on-the-fly strategies mentioned in "Introduction", which takes advantage of the high dynamic performance of the galvanometric scanner but ignores the potential advantage of its working area. Besides, the on-the-fly method using geometric shrinkage and arc transition is the proposed new on-the-fly strategy, which upgrades the major strategies and overcomes the shortcomings of them. All experimental groups were repeated five times and the averages were calculated as the final results of each group. The generated platform motion trajectories of three groups are shown in Fig. 6b–d. Remarkably, all groups were

Fig. 5 An experimental setup for **a** on-the-fly laser processing and **b** measuring
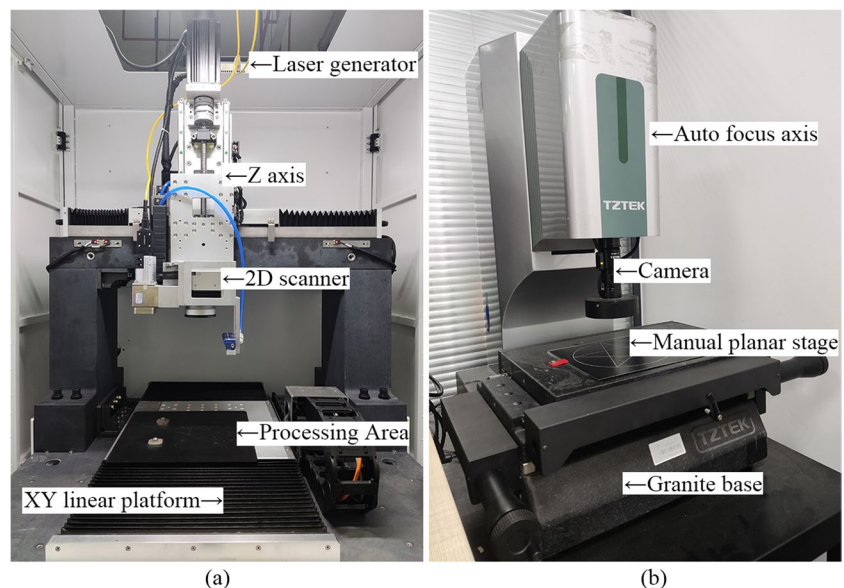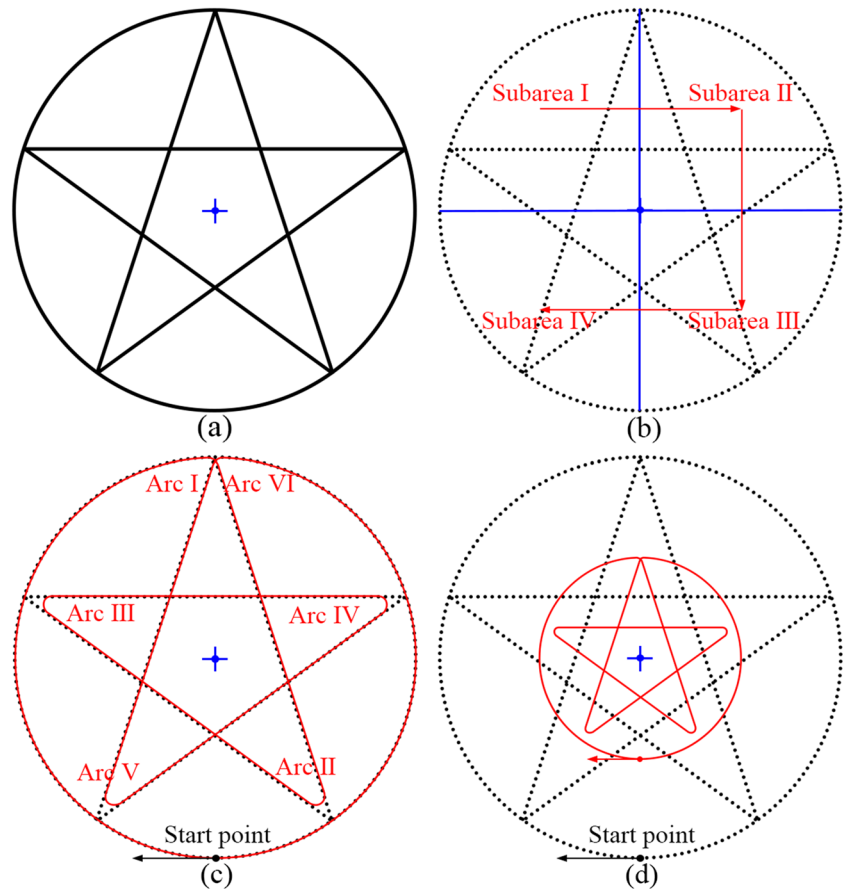

(a)　　　(b)

Fig. 6 **a** Original pattern. **b** Trajectories of the step-and-scan method. **c** Trajectories of the on-the-fly method using arc transition only. **d** Trajectories of the on-the-fly method using geometric shrinkage and arc transition. Black marks the target trajectories, red marks the platform trajectories, and blue marks the reference lines

performed with the same velocity and acceleration of the platform, 100 mm/s and 1000 mm/s², respectively. And the same correction for the scanner's graphic distortion was applied for the three groups. In the step-and-scan method, the working velocity and acceleration of the scanner were set to 100 mm/s and 1000 mm/s², respectively, and the jump delay was set to 1 ms.

The laser processed samples from the three groups are displayed in Fig. 7a. The intersection edges of the subareas in the step-and-scan method were analyzed by comparison with the on-the-fly method, selectively magnified, and observed with the VMA Video Measuring Machine. Figure 7b–g highlights the presence of stitching errors and overburn defects in the step-and-scan method, leading to discontinuity and quality loss. Conversely, the on-the-fly method exhibits none of these defects.

The total processing time of each group is listed in Table 1, from which it can be noticed that, in this case, the time span taken by the proposed method (Group III) has been diminished by 67.3% compared to the traditional step-and-scan method (Group I), and 51.4% compared to the major on-the-fly method (Group II). Finally, the accuracy of the three groups was detected quantitatively by the VMA Video Measuring Machine. The roundness errors

of circles are shown in Fig. 8, and the straightness errors of star lines are shown in Fig. 9. The detected processing errors of all groups are basically close and satisfy the requirement, which means that the proposed method can enhance productivity without compromising precision.

Figures 10, 11, and 12 illustrate the position and velocity of each axis in the galvanometric scanner as a function of time, according to the three groups of categories. By comparison between Figs. 10 and 11, the step-and-scan method exploits the characteristic of the scanner working area extensively (− 45 to 45 mm), while in the on-the-fly method using transition only, the range of movement of both axes is significantly smaller (− 7.5 to 7.5 mm, approx.) and the scanner remains motionless (velocity = 0) most of the processing time. However, the maximal velocity of Fig. 11 (641.7 mm/s) is much greater than that of Fig. 10 (100 mm/s), taking advantage of the high dynamic performance of the galvanometers. The proposed method shown in Fig. 12 combines the advantages of the methods in both Figs. 10 and 11 which refer to full utilization of the working area and fast response of the galvanometric scanner. In Fig. 12, the motion range of the axes is also − 45 to 45 mm, but the maximal velocity reaches 1226.9 mm/s. That exactly gives the reason why the proposed method achieves the optimal time.

Fig. 7 **a** Processed sample and some defects of **b, d** stitching error and **f** overburn in the step-and-scan method compared to **c, e, g** the same regions in the on-the-fly method. Blue, pink, and green mark three magnified regions located on the intersection edges
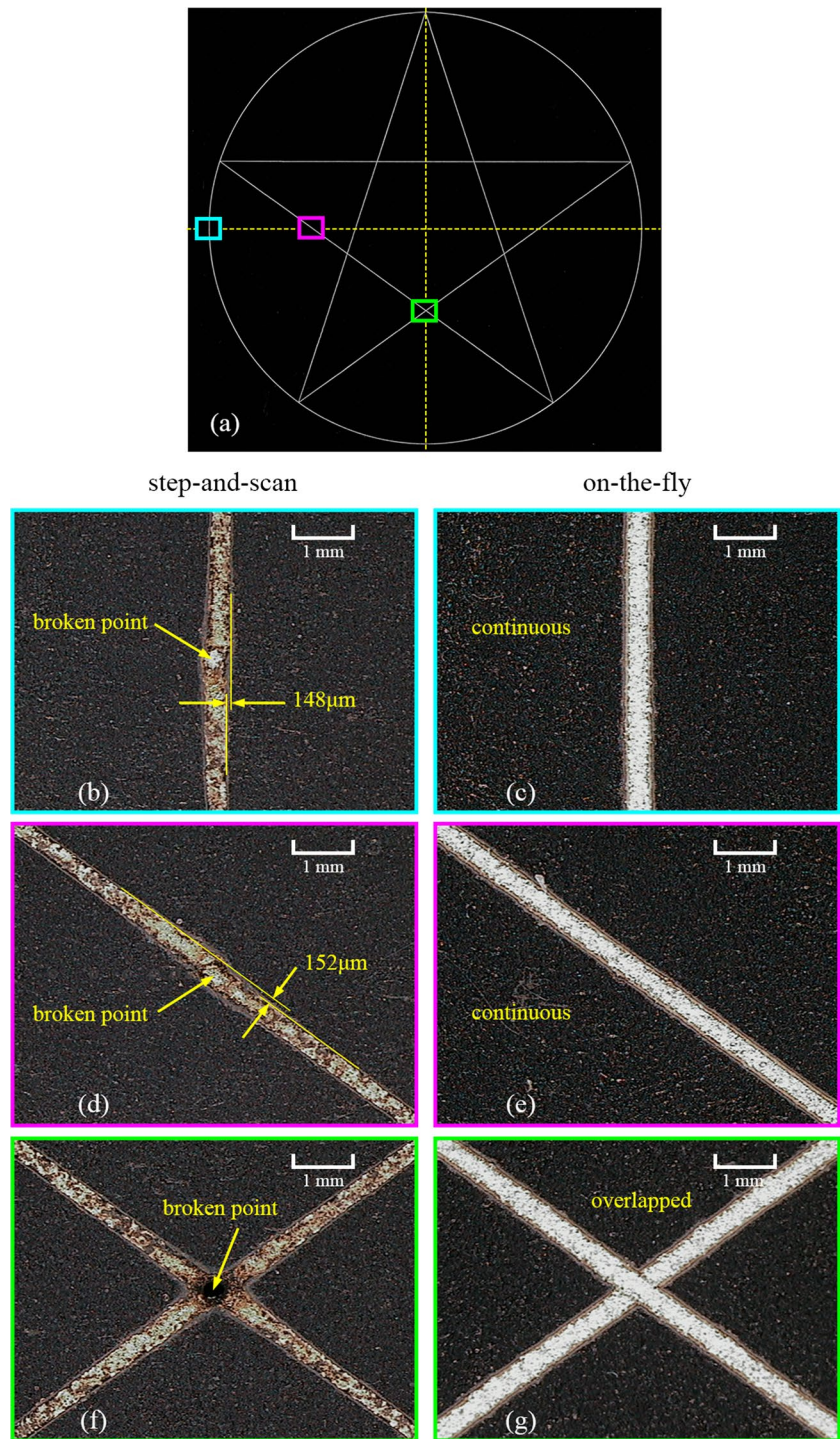
4 Conclusions

This study has developed a new on-the-fly laser processing method to improve efficiency for continuous large-scale trajectories. It utilizes the characteristic of the scanner working area by performing geometric shrinkage and achieves high dynamic performance of the scanner by smoothening trajectories with transitional arcs. Decomposed trajectories,

Table 1 Measurement of total processing time. Group I refers to the step-and-scan method, Group II refers to the on-the-fly method using arc transition only, and Group III refers to the on-the-fly method using geometric shrinkage and arc transition

	Group I	Group II	Group III
Processing time (sec)	20.5	13.8	6.7
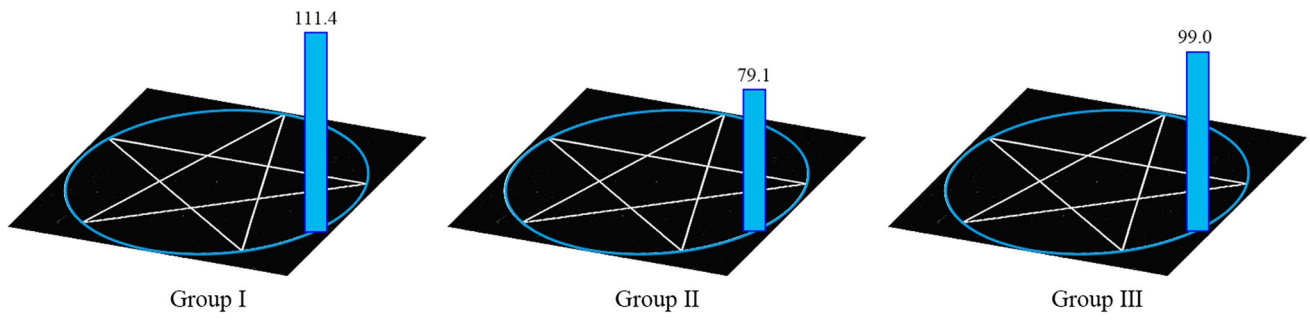
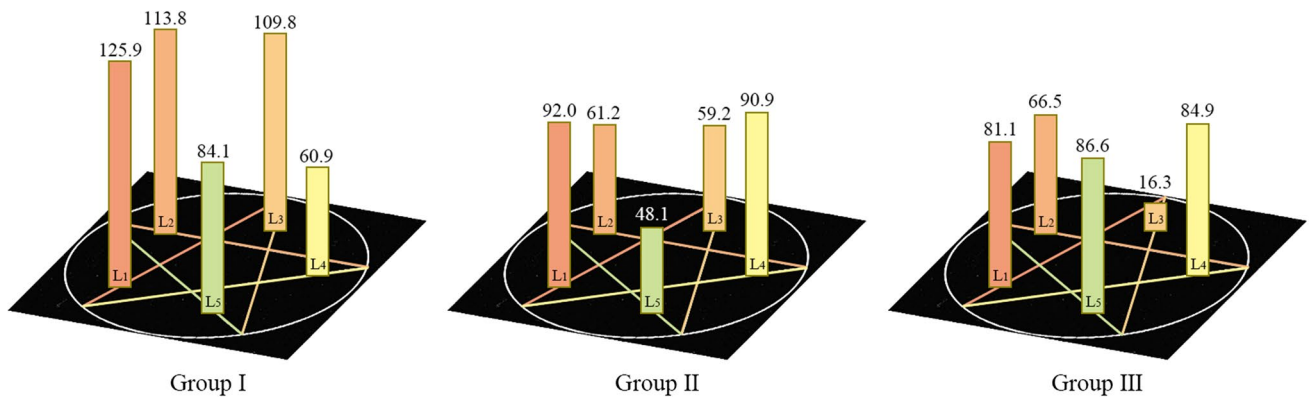**Fig. 8** Measurement of roundness errors of circles (unit μm)

Fig. 9 Measurement of straightness errors of star lines (unit μm). L1, L2, L3, L4, and L5 refer to five linear edges of the star

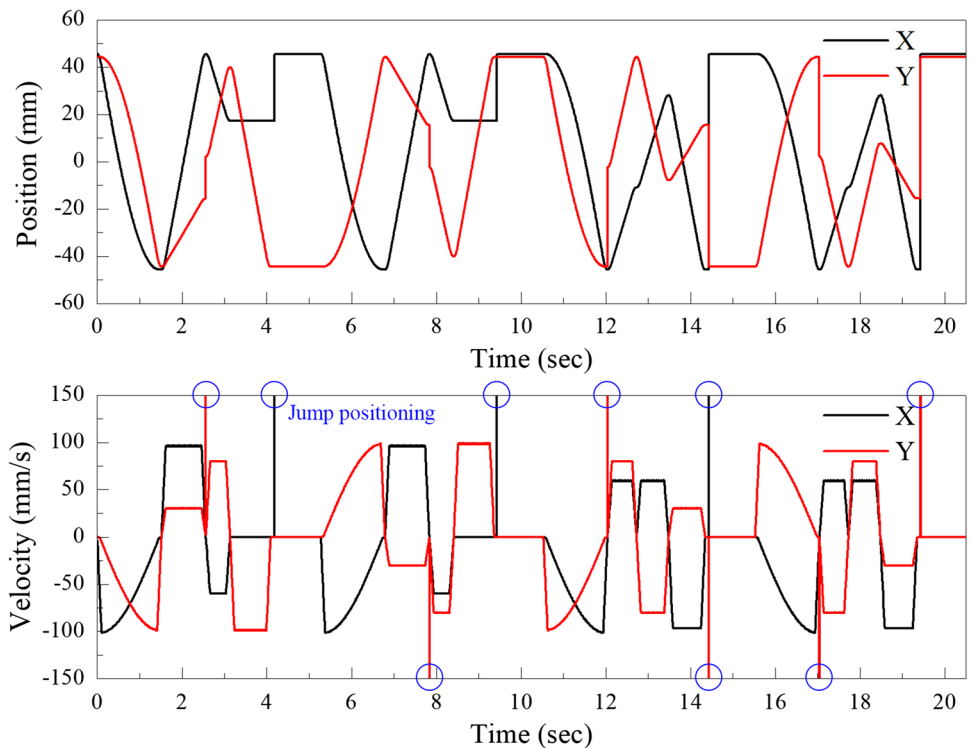**Fig. 10** Variations of the position and velocity of the scanner *XY* axis using the step-and-scan method (Group I)

Fig. 11 Variations of the position and velocity of the scanner *XY* axis using the on-the-fly method with transition only (Group II)
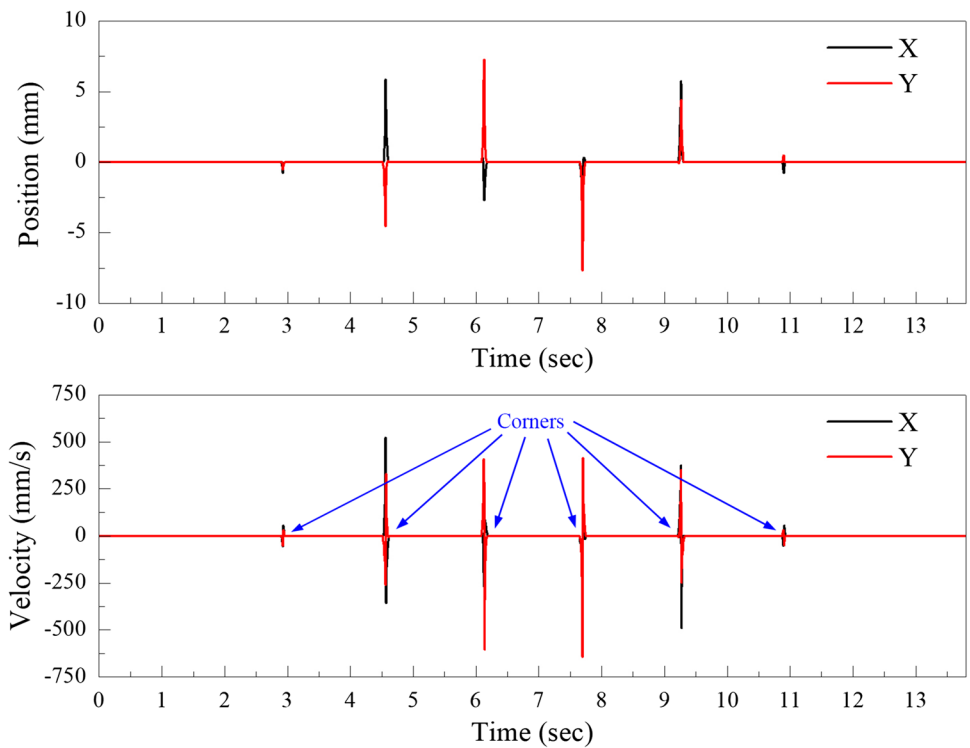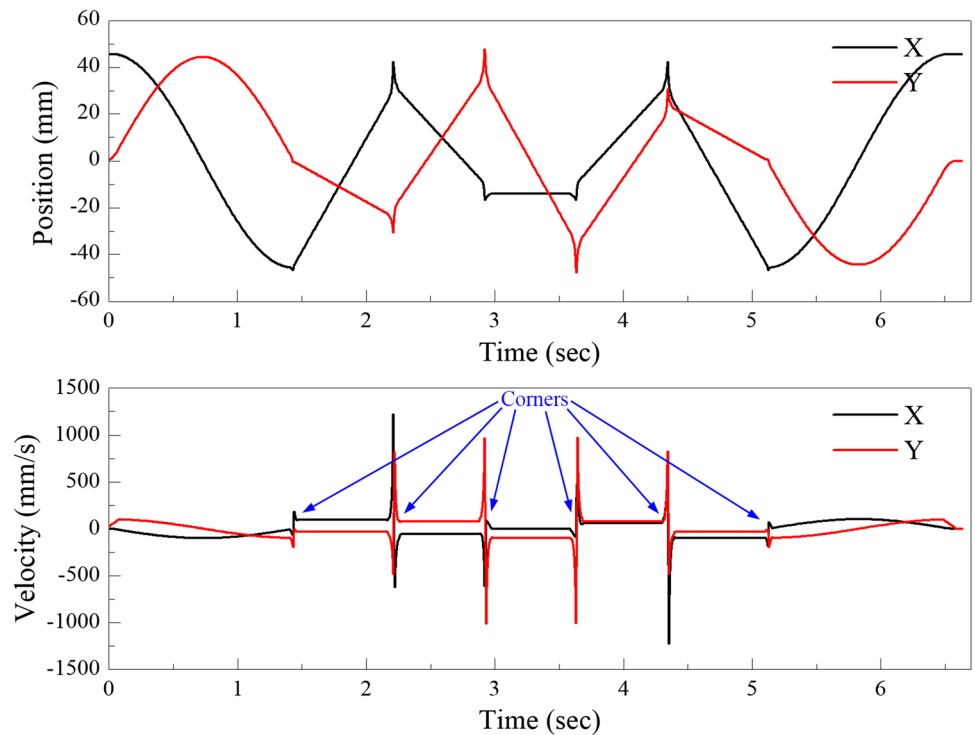

Fig. 12 Variations of the position and velocity of the scanner *XY* axis using the on-the-fly method with shrinkage and transition (Group III)

applied to platform motion, are derived from target trajectories firstly, and then, vector subtraction of positions is implemented to obtain motion interpolation of the scanner in real-time context. The proposed method takes advantages of both higher productivity and less calculative burden.

Experimental results with the given patterns indicate that the total processing time of the proposed method is reduced by 67.3% compared with the traditional step-and-scan method, and 51.4% compared with the major on-the-fly method. Moreover, no defect of stitching error or overburn appears,

and all detected errors satisfy the requirement. Analysis on the variations of positions and velocities can validate and demonstrate the features of this proposed method as well.

Declarations

Conflict of interest The authors declare no competing interests.

References

1. Uzunoglu E, Dede MIC, Kiper G (2016) Trajectory planning for a planar macro-micro manipulator of a laser-cutting machine. Ind Robot 43:513–523. https://doi.org/10.1108/IR-02-2016-0057
2. Jiang M, Jiang Y, Zeng XY (2008) Scanning path planning for graphics objects in laser flying marking system. Opt Eng 47:94302–94306. https://doi.org/10.1117/1.2978952
3. Kang H, Suh J, Kwak SJ (2011) Welding on the fly by using laser scanner and robot. IEEE, pp 1688–1691
4. Stoesslein M, Axinte D, Gilbert D (2016) On-the-fly laser machining: a case study for in situ balancing of rotative parts. J Manuf Sci Eng 139(3):31002. https://doi.org/10.1115/1.4034476
5. Chen D, Wang P, Pan R, Zha C, Fan J, Kong S, Li N, Li J, Zeng Z (2021) Research on in situ monitoring of selective laser melting: a state of the art review. Int J Adv Manuf Technol 113:3121–3138. https://doi.org/10.1007/s00170-020-06432-1
6. Yung KC, Choy HS, Xiao T, Cai Z (2021) UV laser cutting of beech plywood. Int J Adv Manuf Technol 112:925–947. https://doi.org/10.1007/s00170-020-06376-6
7. Diaci J, Bračun D, Gorkič A, Možina J (2011) Rapid and flexible laser marking and engraving of tilted and curved surfaces. Opt Lasers Eng 49:195–199. https://doi.org/10.1016/j.optlaseng.2010.09.003
8. Buser M, Onuseit V, Graf T (2021) Scan path strategy for laser processing of fragmented geometries. Opt Lasers Eng 138:106412. https://doi.org/10.1016/j.optlaseng.2020.106412
9. Kim K (2012) Laser scanner-stage synchronization method for high-speed and wide-area fabrication. J Laser Micro Nanoeng 7:231–235. https://doi.org/10.2961/jlmn.2012.02.0018
10. Kim K, Yoon K, Suh J, Lee J (2011) Laser scanner stage on-the-fly method for ultrafast and wide area fabrication. Phys Procedia 12:452–458. https://doi.org/10.1016/j.phpro.2011.03.156
11. Cui M, Lu L, Zhang Z, Guan Y (2021) A laser scanner–stage synchronized system supporting the large-area precision polishing of additive-manufactured metallic surfaces. Engineering 7:1732–1740. https://doi.org/10.1016/j.eng.2020.06.028
12. Erkorkmaz K, Alzaydi A, Elfizy A, Engin S (2014) Time-optimized hole sequence planning for 5-axis on-the-fly laser drilling. CIRP Ann 63:377–380. https://doi.org/10.1016/j.cirp.2014.03.126
13. Yoon K, Kim K, Lee J (2014) One-axis on-the-fly laser system development for wide-area fabrication using cell decomposition. Int J Adv Manuf Technol 75:1681–1690. https://doi.org/10.1007/s00170-014-6267-8
14. Alzaydi A (2018) Trajectory generation and optimization for five-axis on-the-fly laser drilling: a state-of-the-art review. Opt Eng 57:1. https://doi.org/10.1117/1.OE.57.12.120901
15. Alzaydi A (2019) Time-optimal, minimum-jerk, and acceleration continuous looping and stitching trajectory generation for 5-axis on-the-fly laser drilling. Mech Syst Signal Process 121:532–550. https://doi.org/10.1016/j.ymssp.2018.11.045